

Supporting Information

Zinc and Cadmium thioamidate complexes: Rational design of single-source precursors for the AACVD of ZnS

Max E. Robson^{a,b} and Dr Andrew L. Johnson^{a*}

* Corresponding Author

a: Department of Chemistry, University of Bath, Claverton Down, Bath, BA2 7AY, U.K.

b: Centre of Doctoral Training in Aerosol Science, University of Bristol, School of Chemistry,
Cantock's Close, BS8 1TS, UK.

Contents

General Experimental	2
Synthesis and analysis of $[\text{Zn}\{\text{OC}(\text{iPr})\text{N}^t\text{Bu}\}_2]_2$	3
NMR studies	3
Crystallographic analysis of $[\text{Zn}\{\text{OC}(\text{iPr})\text{N}^t\text{Bu}\}_2]_2$	4
Thermogravimetric analysis of $[\text{Zn}\{\text{OC}(\text{iPr})\text{N}^t\text{Bu}\}_2]_2$	5
X-ray Crystallography data	7
Diffusion ordered NMR spectra.....	8
¹ H NMR spectra of by-products from pyrolysis of compound 3	16
Energy Dispersive X-Ray spectroscopy Data.....	17

Supporting Information

General Experimental

Chemical reagents were provided by Sigma Aldrich, Fisher Scientific, Alfa Aesar or FluoroChem and used without further purification. Reactions were conducted under inert conditions, using standard Schlenk line and glovebox techniques using an Argon atmosphere. Only thioamide and amide compounds were stored in ambient conditions, with all other compounds stored under argon. All solvents were dried under argon using an Innovative Technologies solvent purification system, then degassed using cold vacuum degassing (77 K) and argon. THF and diethyl ether were dried by refluxing over either sodium or potassium in the presence of benzophenone and were subsequently degassed twice using cold vacuum degassing. All solvents were stored in J Youngs ampules over activated molecular sieves. Metal amide reagents were prepared according to methods reported in the literature.

NMR experiments were carried out using J Youngs valve NMR tubes prepared in a glovebox. NMR data was collected at 25 °C using either a Bruker Avance AV-400 or Avance II+ AV-500 spectrometer. DOSY experiments were carried out using a standard double attenuated echo sequence with longitudinal eddy current delay. Experiments were typically carried out with a gradient strength ranging from 10% to 90% using smoothed square gradients, and with D and d set to 50 ms and 2 ms respectively. Data was processed using Bruker Dynamics Centre.

High resolution mass spectrometry (HRMS) results were acquired on an externally calibrated Agilent QTOF UHR-ToF mass spectrometer coupled to an electrospray source (ESI-QToF). Molecular ions were detected as their protonated adduct, $[M+H]^+$.

Elemental analysis was performed under inert conditions by the elemental analysis service at the Science Centre, London Metropolitan University, UK using Dumas combustion method.

Single crystal X-ray diffraction data were collected at 150 K using either a Nonius Kappa CCD, an Agilent Xcalibur or an Agilent SuperNova Dual diffractometer with either Mo-K α ($\lambda = 0.71073 \text{ \AA}$) or Cu-K α ($\lambda = 1.5418 \text{ \AA}$) radiation. The data collected by the diffractometers were processed using the proprietary Nonius or Agilent software. Structures were solved by full-matrix least squares refinement using either the WinGX-170 suite of programs or the programme suite X-SEED. All structural data were obtained by the author or Dr Andrew Johnson with structure refinement performed by the author, Dr Andrew Johnson or Dr Gabriele Kociok-Köhn (Material and Chemical Characterisation Facility, at the University of Bath).

Aerosol-assisted chemical vapour depositions were conducted using a hot wall furnace system combined with a TSI 3076 Constant Output Atomiser. Argon was used as a carrier gas at a flow rate between 1.5 and 2.0 L/min. Dried and degassed THF was used as the solvent, and each precursor solution was prepared in a glovebox. The precursor pot was sealed under argon, removed and attached to the AACVD rig. Square FTO-coated glass substrates (largest dimension *ca.* 2 cm) were washed via sonication in 1:1:1 solution of Di water, acetone and *iso*-propanol and dried before cleaning with an O₂ plasma. Four of these were placed in the main flux of the deposition furnace. Before deposition, argon gas was flushed through the chamber (by-passing the precursor pot) for 1 hour to create an inert atmosphere, while the furnace warmed to the appropriate temperature. Subsequently, taps of the precursor solution pot were opened to allow deposition for 45 minutes. After deposition, the taps were closed, and the furnace was allowed to cool under argon before removal and analysis of the film samples.

Deposition conditions used in AACVD reactions are shown in Table S1

Supporting Information

Film	Conc. of 3 (THF)/ mol dm ⁻³	Reactor Temp./ °C	Deposition time /min
A	0.1	175	45
B	0.1	200	45
C	0.1	250	45
D	0.1	300	45
E	0.1	350	45

Table S1. Deposition conditions used for AACVD of thin films using compound **3**.

Powder X-Ray Diffraction (PXRD) patterns were collected on either a Bruker AXS D8 Advance (Cu-K α radiation, $\lambda = 1.5418 \text{ \AA}$) or a Stoe Stadi P (Cu-K α radiation, $\lambda = 1.54056 \text{ \AA}$) diffractometer in flat plate mode at 298 K. Results were analysed in EVA, Excel and WinXPOW.

Raman spectra were recorded on a Renishaw inVia system using either a 532 nm (green) or 785 nm (UV- HeCd) laser, at varying energy intensity and exposure times. The data was processed using the associated Renishaw WiRE software package. All experiments were run by personnel at the Material and Chemical Characterisation Facility, at the University of Bath, with direction from the author.

FESEM images were taken using a Jeol 6301F or JEOL JSM-7900F field effect scanning electron microscope. An accelerating voltage of 5.0 kV was kept constant throughout the analysis. Samples were desiccated for 24 hours prior to analysis. All experiments were run by personnel at the Material and Chemical Characterisation Facility, at the University of Bath, with direction from the author.

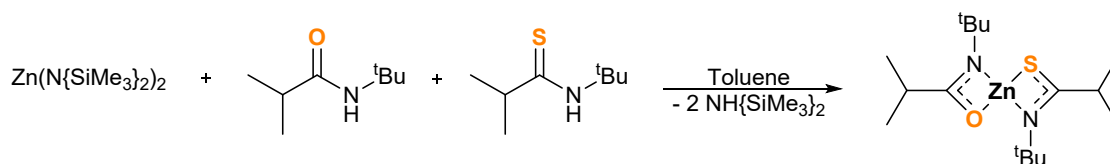
EDX analysis was performed using an JOEL JSM-IT300 scanning electron microscope (WD10mm and 15kV) with an Oxford Instruments X-max 80 (EDX) spectrometer. All EDX experiments were conducted at the University of Bristol by Jean-Charles Eloi.

Synthesis and analysis of $[\text{Zn}(\text{OC}\{i\text{Pr}\}\text{N}^t\text{Bu})_2]_2$

A preliminary investigation into zinc oxysulfide film formulation was conducted based on the success of the zinc thioamidates. The Zn(O,S) precursor was designed as a combination of the ligand $[\text{L}^2]$ and its oxygen-based amidate derivative $[\text{OC}\{i\text{Pr}\}\text{N}^t\text{Bu}]^-$ ($[\text{L}^5]$), as the heteroleptic compound $(^t\text{BuN}\{i\text{Pr}\}\text{CO})\text{Zn}(\text{SC}\{i\text{Pr}\}\text{N}^t\text{Bu})$ – see Scheme S 1. This was targeted via a 1:1:1 reaction of $[\text{Zn}(\text{N}\{\text{SiMe}_3\}_2)_2]$, $\text{H}[\text{L}^2]$ and $\text{H}[\text{L}^5]$.

Supporting Information

Scheme S 1. Synthesis of $Zn[L^2][L^5]$ using equal parts $Zn(N\{SiMe_3\}_2)_2$, amide $H[L^5]_2$ and thioamide $H[L^2]$.



Analogous to the zinc *bis*-thioamidate synthesis, the reaction was conducted at room temperature in toluene. Upon combination of $H[L^2]$ and $[Zn(N\{SiMe_3\}_2)_2]$, a colourless precipitate dropped out, presumed to be the intermediate $(Me_2Si)_2NZn[L^2]$. After 30 minutes, one equivalent of the amide $H[L^5]$ was added which triggered complete redissolution of the precipitate within 1 minute. After another 30 minutes, the solution was concentrated *in vacuo*, from which colourless crystals grew at 5°C and were isolated.

NMR studies

In deuterated benzene- d_6 , a sample of the crystalline material was analysed via 1H and ^{13}C NMR spectroscopy.

From 1H NMR spectroscopy, no resonance peaks could be reasonably attributed to neither {N-H} moiety, nor a hexamethyl disilazane $[N(SiMe_3)_2]$ component. The proton environments of each ligand were expected to be of different chemical shifts and, therefore, resolvable from one another. However, only 3 proton environments could be observed corresponding to the *iso*-propyl (δ_H : h, 2.79 and d, 1.27 ppm) and *tert*-butyl (δ_H : 1.32 ppm) moieties. These resonance peaks differed from those of the ZnS precursor $Zn[L^2]_2$ (δ_H : 2.86, 1.24 and 1.16 ppm).

In a similar vein, only five carbon environments were detected using ^{13}C NMR spectroscopy. These included one deshielded resonance peak at δ_C : 184.2 ppm, attributed to a new [N-C-E] carbon environment. However, this was the only deshielded carbon environment, rather than the expected two, and was not in close correspondence with that of compound **3**, $Zn[L^2]_2$ (δ_C : 207.2 ppm).

This crystalline compound was grown from the reaction mixture of $[Zn(N\{SiMe_3\}_2)_2]$, $H[L^2]$ and $H[L^5]$ in toluene. After its isolation, the liquor was reduced *in vacuo* and a secondary batch of crystalline solid was grown, on which a 1H NMR spectroscopy study was also conducted. This second yield was found to contain the same three resonance peaks as the compound first crystallised (δ_H : 2.79, 1.32 and 1.27 ppm) and additional resonance peaks corresponding to $Zn[L^2]_2$ (δ_H : 2.86, 1.24 and 1.16 ppm) in approximately equal ratio. A third crystallisation from the liquor was found to contain the same proton resonances with a far greater excess of peaks corresponding with $Zn[L^2]_2$.

These data were not as expected and indicated that two homoleptic species $Zn[L^5]_2$ and $Zn[L^2]_2$ had formed, with the former first to crystallise out of toluene. This was confirmed via X-ray crystallographic studies.

Crystallographic analysis of $Zn(OC\{^iPr\}N^tBu)_2$

From the first batch of material crystallised from toluene, a sample sufficient for X-ray analysis was isolated. The structural identity of this compound confirmed the formation of the homoleptic zinc *bis*-amidate compound $Zn[L^5]_2$ (**6**) and is presented in Figure S 1.

Compound **6** crystallised as a dimer in the space group *Pbca*. The unit cell comprised a zinc centre with one chelating and one bridging amidate ligand. From this $Zn[L^5]_2$ unit the symmetry operator -

Supporting Information

$x+1, -y+1, -z+1$ could be used to complete the dimer. This resulted in the formation of three four-membered rings fused by a $\{Zn_2O_2\}$ ring in a strained chair-like conformation. The ligands $[L^2]$ assumed a transoidal arrangement which was packed into a cisoidal pattern of $Zn[L]_2$ units.

This resulted in a highly distorted five-coordinate geometry about the zinc atom. Both amidate ligands were bound in a κ^2-N,S -fashion, although the $[Zn(1)-O(1)\#]$ distance is far longer than the association between the zinc centre and O(1) (1.9759(10) Å) or O(2) (2.1201(10) Å). The sum of all angles around each N(1), N(2), C(5) and C(13) approached 360°. Additionally, each $\{N-C\}$ and $\{C-O\}$ bond within the chelating moiety was similar: $N(1)-C(5) = 1.3043(19)$ Å compared with $N(2)-C(13) = 1.3101(19)$ Å and $O(1)-C(5) = 1.3067(17)$ Å compared with $O(2)-C(13) = 1.3063(17)$ Å. These structural data were indicative of electron delocalisation within the $\{N-C-O\}$ moiety.

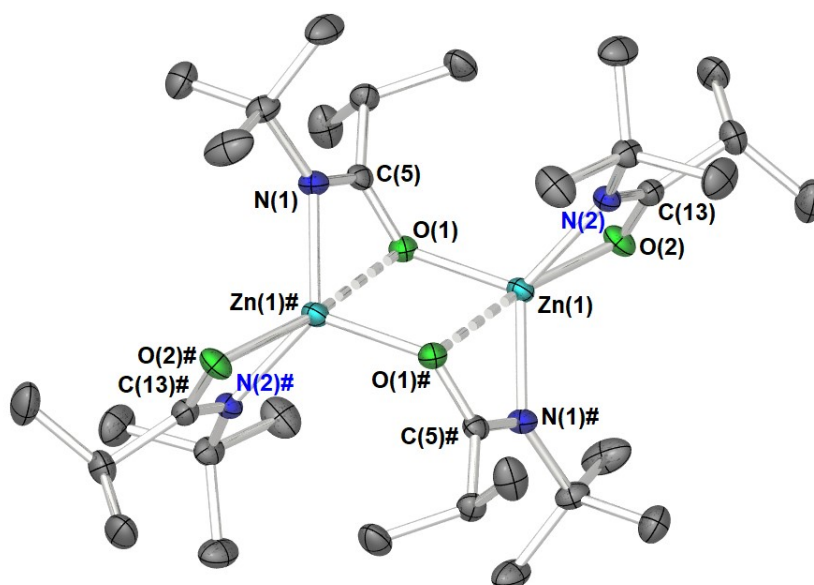
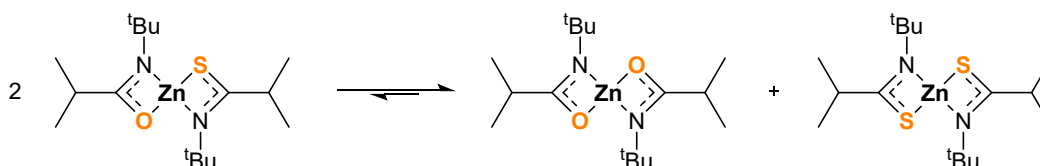


Figure S 1. The molecular structure obtained from the attempted synthesis of $Zn[L^2][L^5]$. Instead, the compound $Zn[L^5]_2$ (6) formed. Thermal ellipsoids are at 50% probability and hydrogen atoms have been omitted. Atoms with '#' labels relate to those in the asymmetric unit cell by the symmetry operator $x+1, -y+1, -z+1$.

This structure was different from that of the sulfide derivative, most notably that it was dimeric, whereas $Zn[L^2]_2$ was monomeric. Presumably, this was to electronically satisfy the oxygen atoms. As a result, the zinc centre was subject to steric strain with the greatest valence angles of $N(1)\#-Zn(1)-N(2) = 124.42(5)^\circ$ and $O(2)-Zn(1)-O(1)\# = 167.15^\circ$, from which $\tau_5 = 0.71$; an apparent preference for a trigonal bipyramidal geometry.

Clearly, the heteroleptic $Zn[L^2][L^5]$ compound had not formed, presumably due to an equilibrium with the two homoleptic zinc *bis*-amidate $Zn[L^5]_2$ and zinc *bis*-thioamidate $Zn[L^2]_2$ species – see Scheme S 1.

Scheme S 2. Suggested equilibrium between the desired heteroleptic $Zn[L^2][L^5]$ (LHS), and the isolated *bis*-amidate $Zn[L^5]_2$ and *bis*-thioamidate $Zn[L^2]_2$ (RHS).



Supporting Information

Thermogravimetric analysis of $\text{Zn}(\text{OC}\{\text{iPr}\}\text{N}^t\text{Bu})_2$

To assess its viability as a single-source precursor to Zn(O,S), thermogravimetric analysis was conducted on $\text{Zn}[\text{L}^5]_2$ – presented in Figure S 1. The thermal profiles of compounds **3** and **6** (described in main publication) are included for comparison.

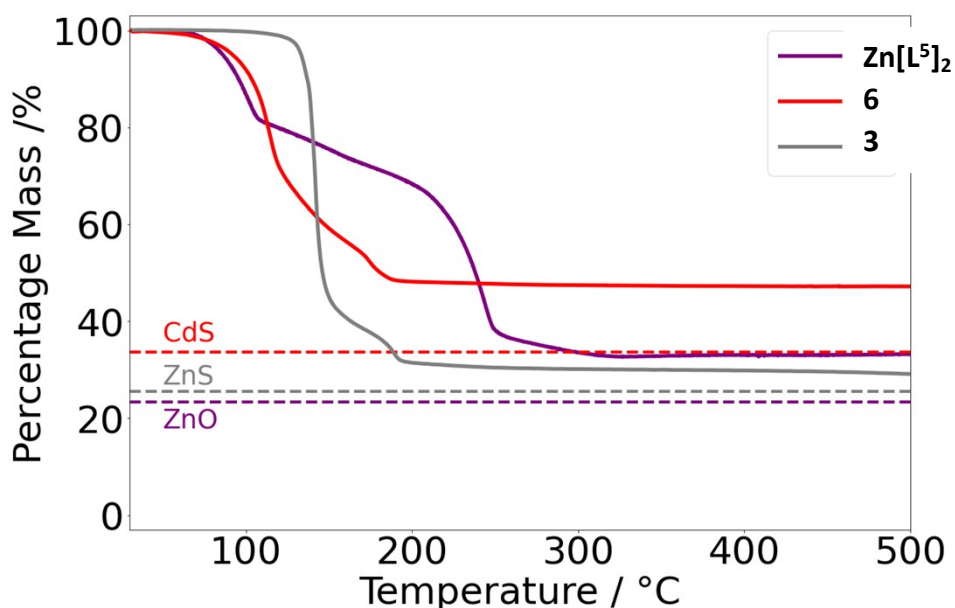


Figure S 2. Thermogravimetric profiles of compound $\text{Zn}[\text{L}^2][\text{L}^5]$ (purple). The thermogravimetric profiles of **3** (grey) and **6** (red) are presented for comparison. The target percentage masses corresponding to ZnO, CdS and ZnS are presented as dotted lines and labelled.

Thermogravimetric data for $\text{Zn}[\text{L}^2][\text{L}^5]$ are presented in the purple plot. Surprisingly, this plot does not follow the profile of its sulfide derivative (compound **3**). A thermal event was first registered between 77°C and 110°C characterised by a 19% mass loss, followed by a secondary event from 110°C to 253°C down to a residual mass of 38%. By 500°C this residual mass had trailed off to 33% which was greater than that of ZnO (23%). Interestingly, the profile of this thermogravimetric data plot was highly reminiscent of the uranium(IV) amidate compound featuring the same ligands $[\text{U}(\text{OC}\{\text{iPr}\}\text{N}^t\text{Bu})_4]$; both precursors exhibited a two-step decomposition process.⁵⁶ This precursor was successfully used to deposit phase-pure UO_2 films via LPCVD. In the light of this, it was suspected that the disparity between target mass and residual mass from pyrolysis of $\text{Zn}[\text{L}^5]_2$ was due to moderate contamination by carbonaceous material.

In comparison to compound **3**, complete decomposition of $\text{Zn}[\text{L}^2][\text{L}^5]$ required higher temperatures (above 250°C). Thus, co-deposition experiments using these compounds should be conducted at temperatures exceeding 250°C.

Supporting Information

X-ray Crystallography data

Table S 2: X-ray crystallographic data relating to compounds **2**, **3**, **4**, **5**, **6** and $[\text{Zn}\{\text{L}^2\}_2]_2$.

Compound	2	3	4	5	6	$[\text{Zn}\{\text{L}^2\}_2]_2$
Chemical formula	C ₂₈ H ₅₆ N ₄ S ₄ Zn ₂	C ₁₆ H ₃₂ N ₂ S ₂ Zn	C ₄₀ H ₄₈ N ₄ S ₄ Zn ₂	C ₄₀ H ₇₂ N ₄ S ₄ Zn ₂	C ₄₈ H ₉₆ Cd ₃ N ₆ S ₆ ·C ₄ H ₈ O	C ₃₂ H ₆₄ N ₄ O ₄ Zn ₂
Formula weight	707.74	381.92	843.8	867.99	1358.97	699.61
Temperature	150.01(10) K	150.00(10) K	150.01(10) K	150.00(10) K	150.00(10) K	150.00(10) K
Wavelength	0.71073 Å	0.71073 Å	0.71073 Å	0.71073 Å	0.71073 Å	1.54184 Å
Crystal system	Monoclinic	Orthorhombic	Monoclinic	Tetragonal	Triclinic	Orthorhombic
Space group	P21/c	Pbcn	P21/n	P41	P-1	Pbca
Unit cell dimensions	a = 11.9996(9) Å b = 10.6361(5) Å c = 14.8354(9) Å α = 90 β = 108.432(7) γ = 90	a = 7.9497(3) Å b = 11.5685(5) Å c = 22.2132(9) Å α = 90 β = 90 γ = 90	a = 9.9334(4) Å b = 17.3065(5) Å c = 12.9808(5) Å α = 90 β = 111.491(9) γ = 90	a = 14.5205(3) Å b = 14.5205(3) Å c = 21.8318(7) Å α = 90 β = 90 γ = 90	a = 11.6481(2) b = 15.5456(4) c = 19.0812(4) α = 91.1994(19) β = 99.1325(16) γ = 101.580(2)	a = 14.01970(10) Å b = 11.84070(10) Å c = 22.47726(19) Å α = 90 β = 90 γ = 90
Volume	1796.3(2) Å ³	2042.86(14) Å ³	2076.41(14) Å ³	4603.1(2) Å ³	3336.94(13) Å ³	3731.29(5) Å ³
Z	2	4	2	4	2	4
Density (calculated)	1.309 Mg/m ³	1.242 Mg/m ³	1.350 Mg/m ³	1.252 Mg/m ³	1.353 Mg/m ³	1.245 Mg/m ³
Absorption coefficient	1.590 mm ⁻¹	1.403 mm ⁻¹	1.389 mm ⁻¹	1.254 mm ⁻¹	1.171 mm ⁻¹	1.866 mm ⁻¹
F(000)	752	816	880	1856	1412	1504
Theta range for data collection	2.882 to 27.553°.	3.109 to 29.285°.	3.225 to 29.776°.	2.957 to 27.473°.	2.944 to 30.421°	3.933 to 73.384
Index ranges	-15<=h<=15, -13<=k<=13, -19<=l<=19	-10<=h<=10, -15<=k<=13, -30<=l<=27	-13<=h<=13, -16<=k<=24, -18<=l<=17	-18<=h<=18, -18<=k<=18, -28<=l<=27	-16<=h<=15, - 21<=k<=21, -26<=l<=26	-13<=h<=17, - 14<=k<=13, -27<=l<=27
Reflections collected	6297	16151	17282	40992	49391	34674
Independent reflections	6297 [R(int) = ?]	2530 [R(int) = 0.0316]	5273 [R(int) = 0.0280]	10126 [R(int) = 0.0607]	17582 [R(int) = 0.0549]	3733 [R(int) = 0.0302]
Completeness to theta = 25.242°	99.80%	99.90%	99.80%	99.80%	99.8 %	100.0 %
Max. and min. transmission	1.00000 and 0.86426	1.00000 and 0.74748	1.00000 and 0.79966	1.00000 and 0.80424	1.00000 and 0.96529	1.00000 and 0.85945
Data / restraints / parameters	6297 / 0 / 181	2530 / 0 / 101	5273 / 0 / 230	10126 / 1 / 460	17582 / 0 / 643	3733 / 0 / 200
Goodness-of-fit on F2	0.879	1.092	1.024	1.074	1.047	1.064
Final R indices [I>2sigma(I)]	R1 = 0.0349, wR2 = 0.0650	R1 = 0.0317, wR2 = 0.0635	R1 = 0.0311, wR2 = 0.0609	R1 = 0.0492, wR2 = 0.1065	R1 = 0.0362, wR2 = 0.0729	R1 = 0.0266, wR2 = 0.0709
R indices (all data)	R1 = 0.0590, wR2 = 0.0673	R1 = 0.0390, wR2 = 0.0662	R1 = 0.0434, wR2 = 0.0653	R1 = 0.0667, wR2 = 0.1192	R1 = 0.0582, wR2 = 0.0827	R1 = 0.0282, wR2 = 0.0719

Supporting Information

Largest diff. peak and hole	0.734 and -0.442 e.Å ⁻³	0.522 and -0.431 e.Å ⁻³	0.336 and -0.277 e.Å ⁻³	0.912 and -0.365 e.Å ⁻³	0.789 and -0.651 e.Å ⁻³	0.451 and -0.373 e.Å ⁻³
CCDC Number	2351132	2351134	2351133	2351135	2351131	2351130

Supporting Information

Diffusion ordered NMR spectra

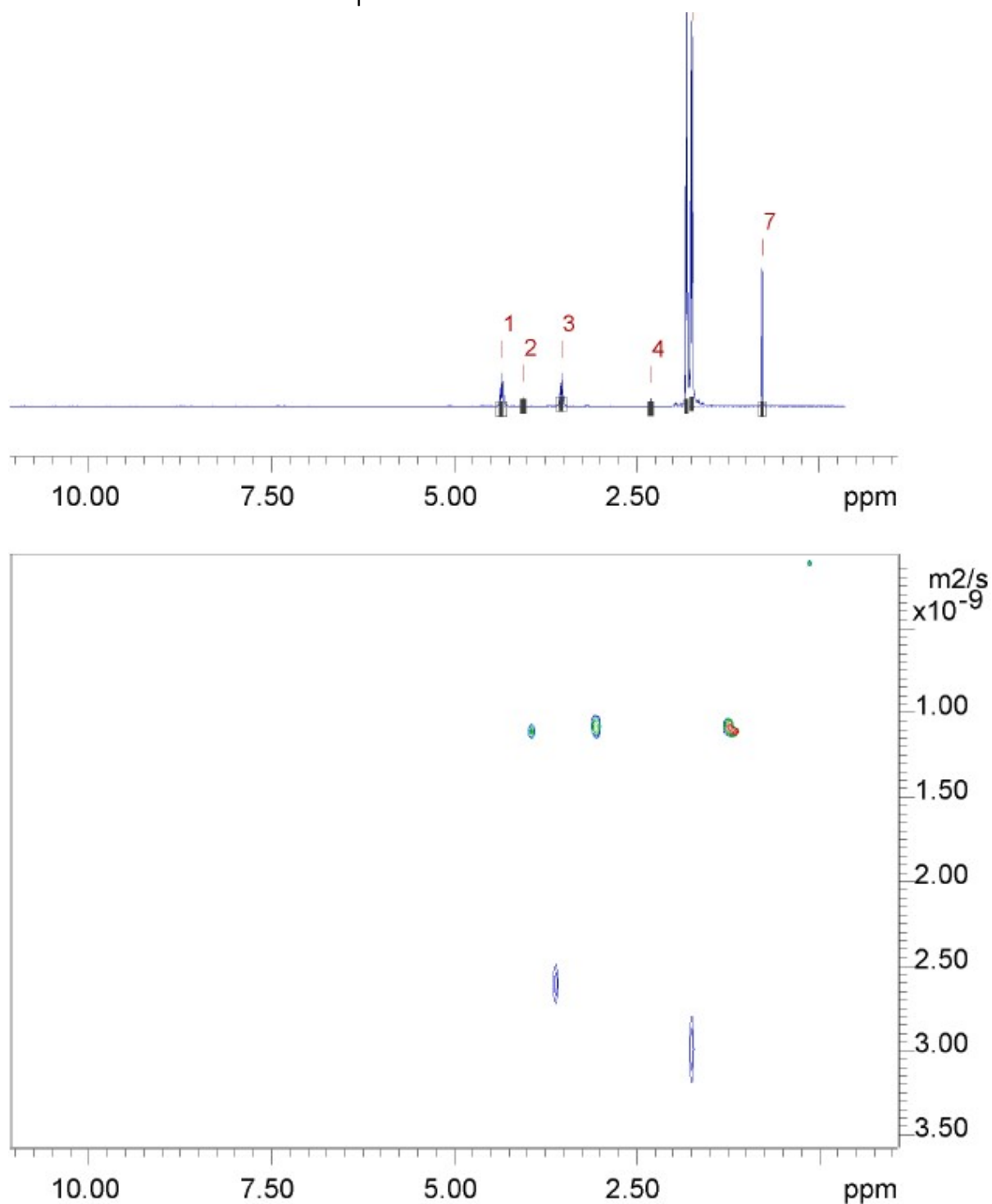


Figure S 3. DOSY spectrum of compound **2** in THF-*d*₈.

Supporting Information

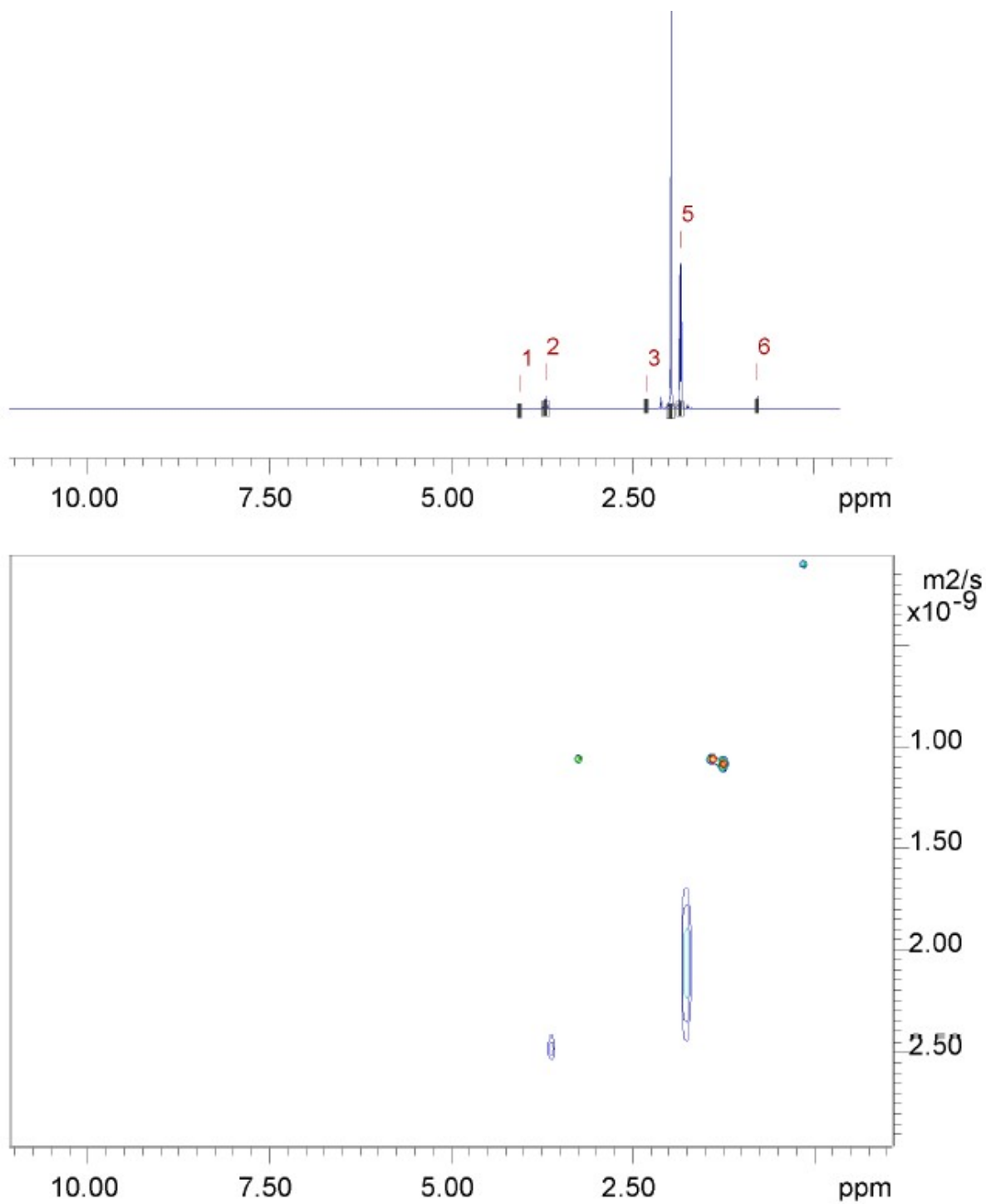
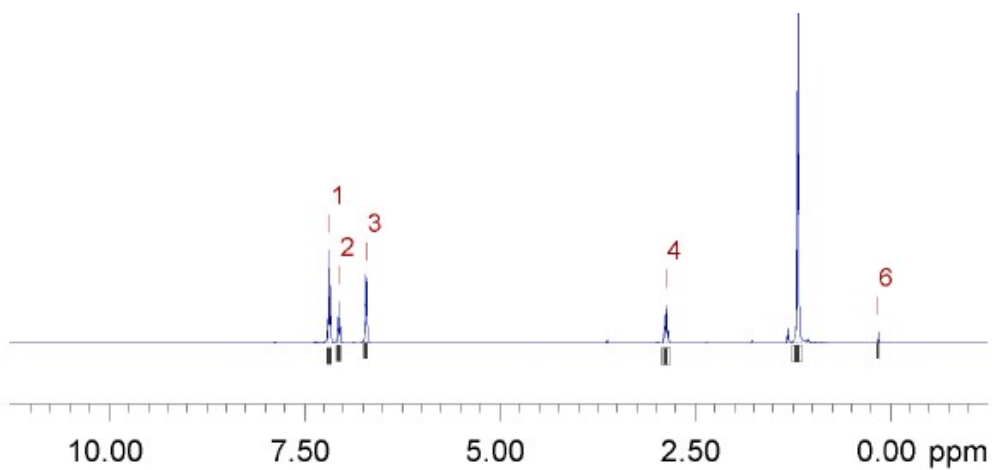


Figure S 4. DOSY spectrum of compound **3** in THF-d₈.

Supporting Information



Dosy/Fit

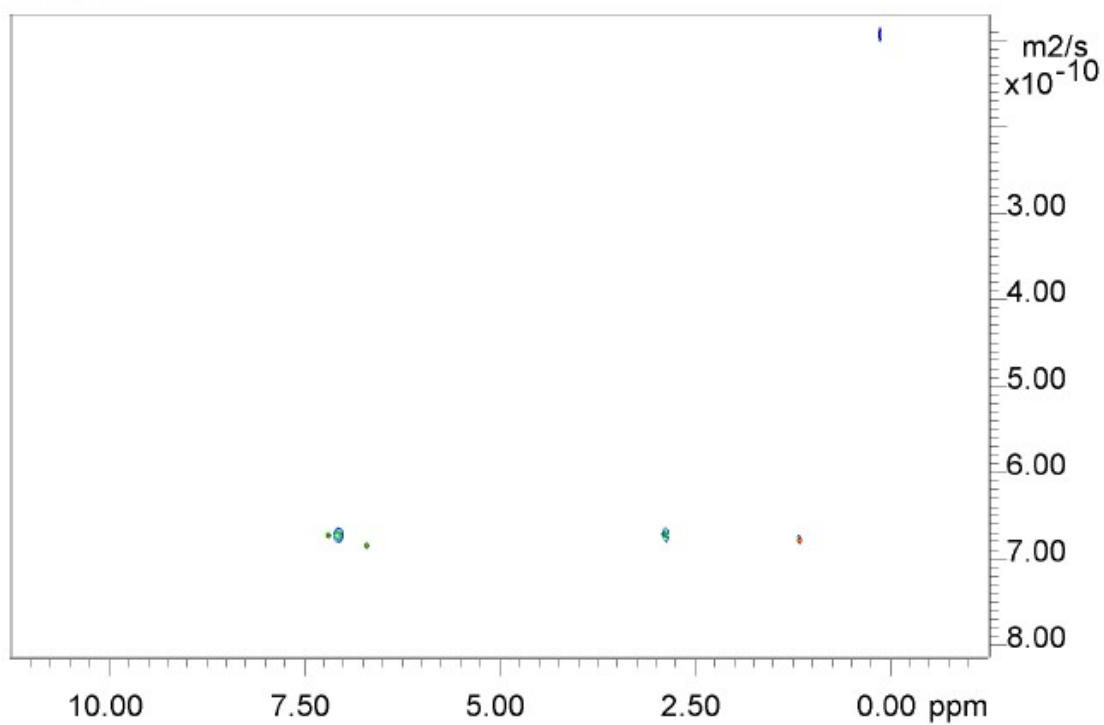
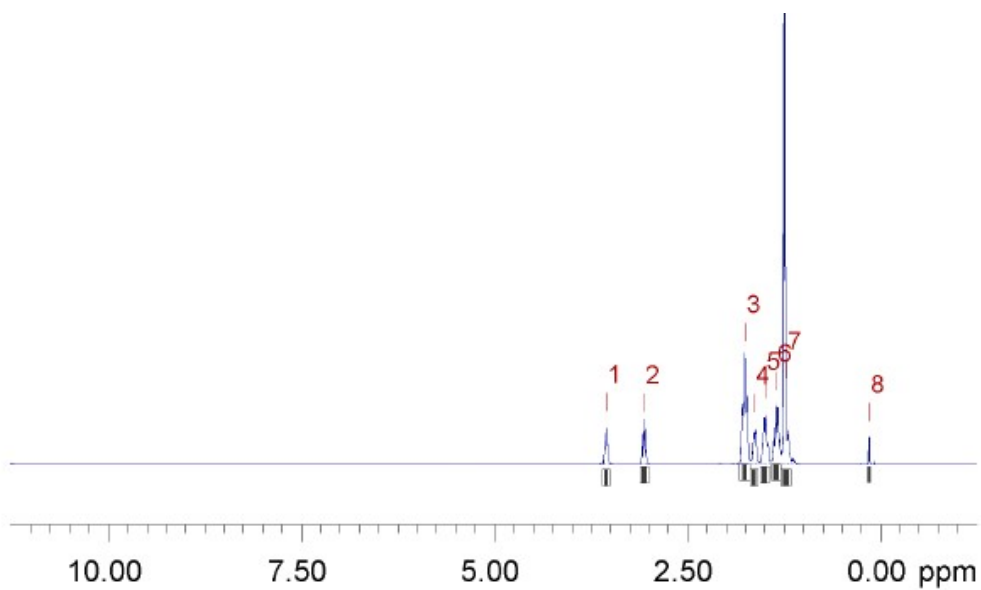


Figure S 5. DOSY spectrum of compound **4** in THF-*d*₈.

Supporting Information



Dosy/Fit

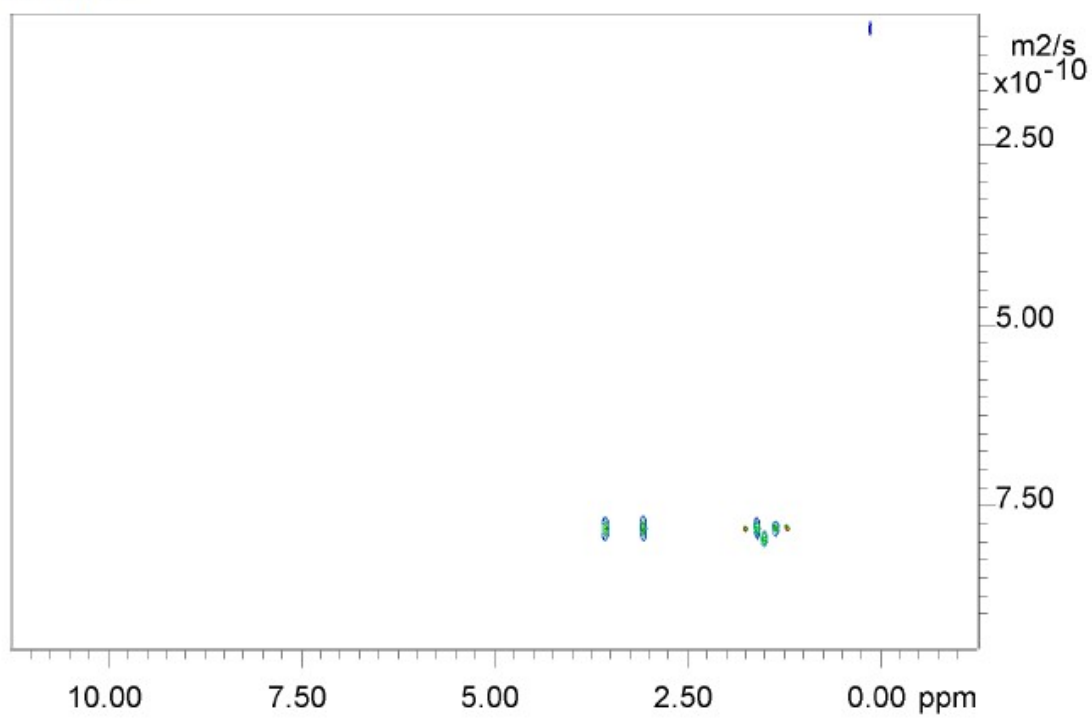
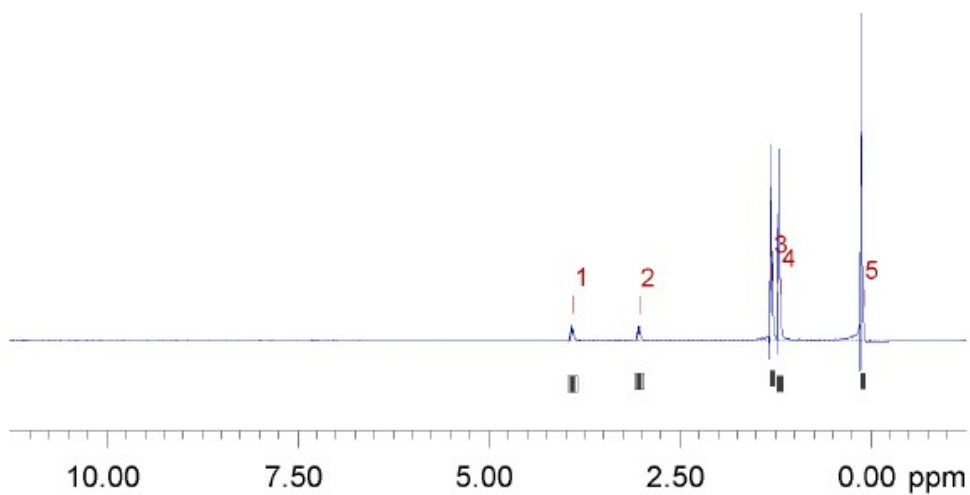


Figure S 6. DOSY spectrum of compound 5 in THF-d₈.

Supporting Information



Dosy/Fit

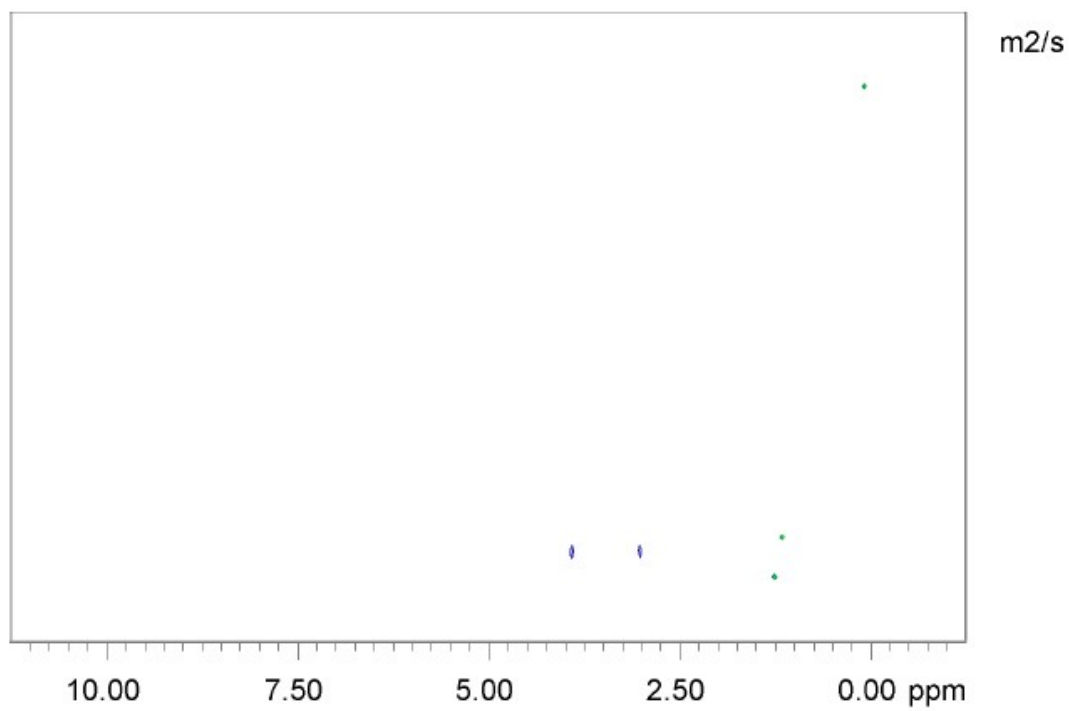
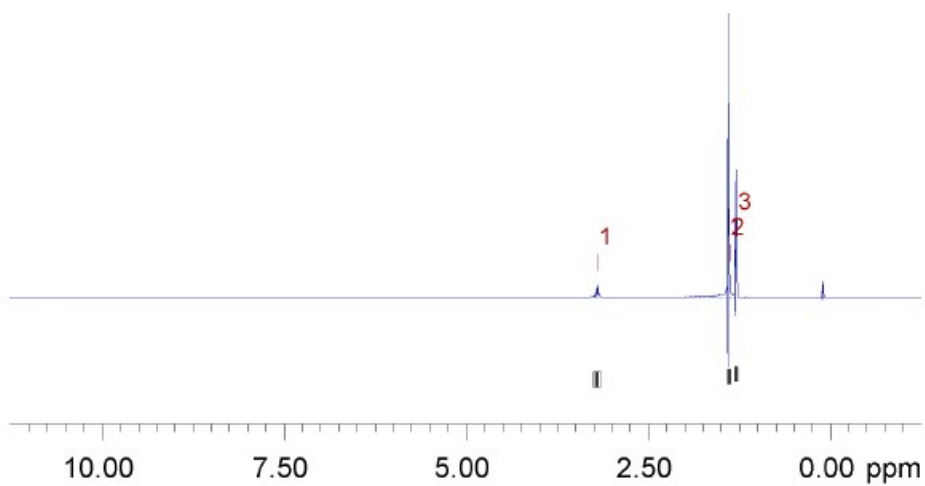


Figure S 7. DOSY spectrum of compound **2** in CDCl₃.

Supporting Information



Dosy/Fit

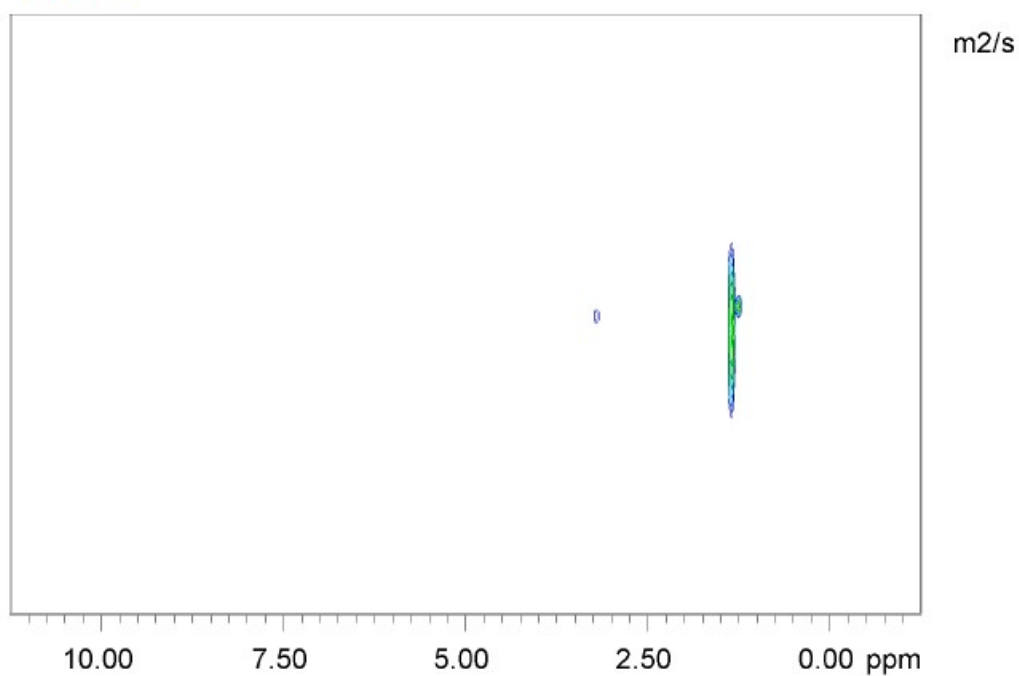
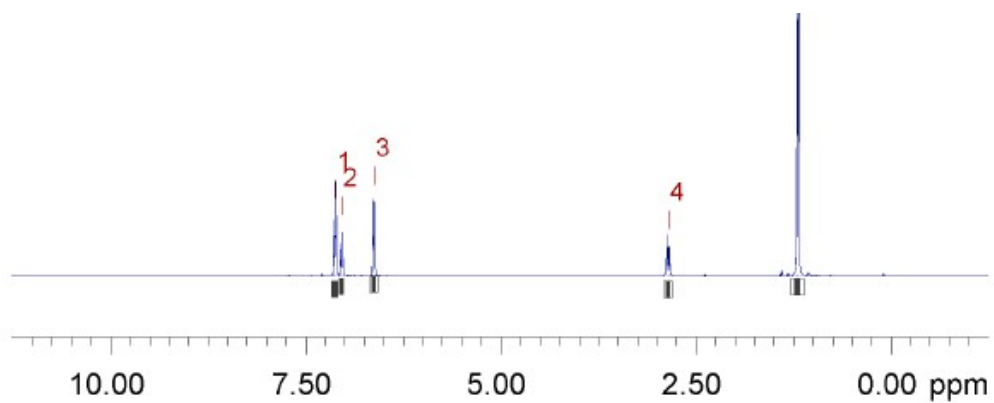


Figure S 8. DOSY spectrum of compound **3** in CDCl_3 .

Supporting Information



Dosy/Fit

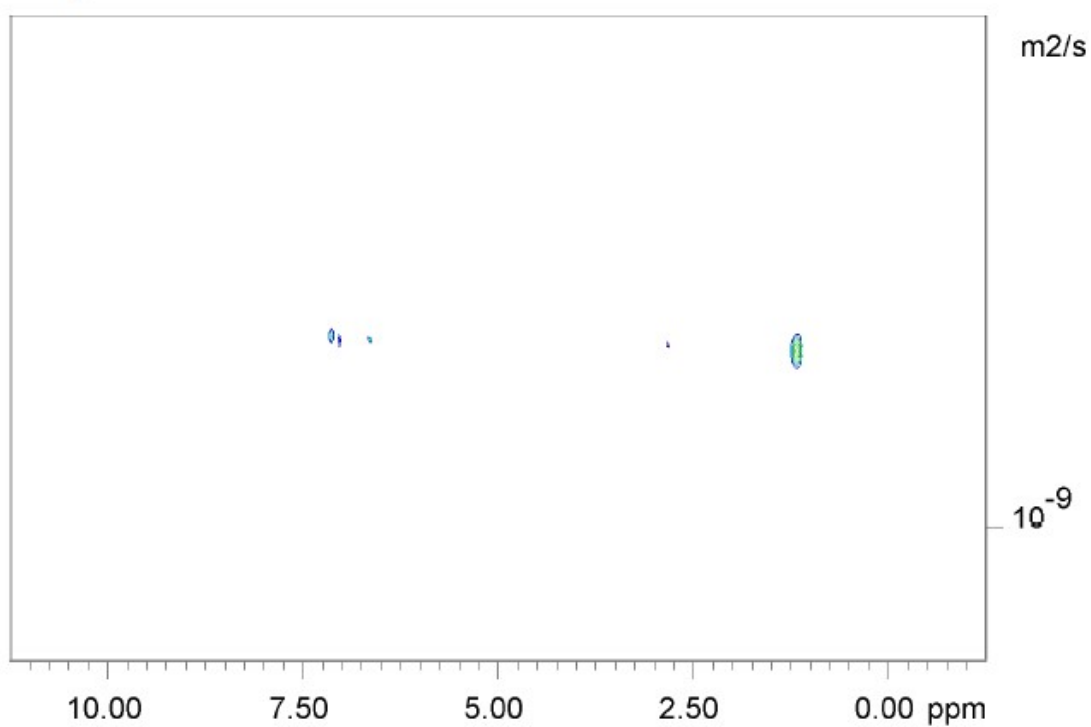
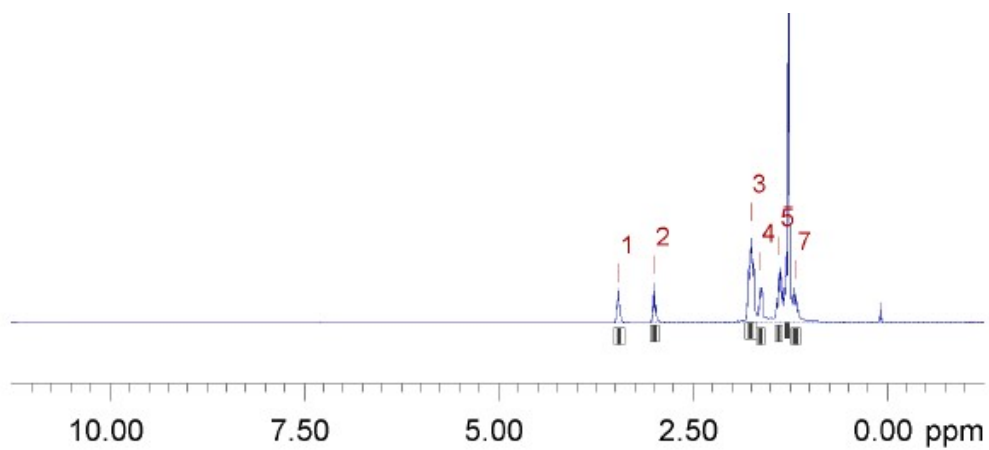


Figure S 9. DOSY spectrum of compound **4** in CDCl₃.

Supporting Information



Dosy/Fit

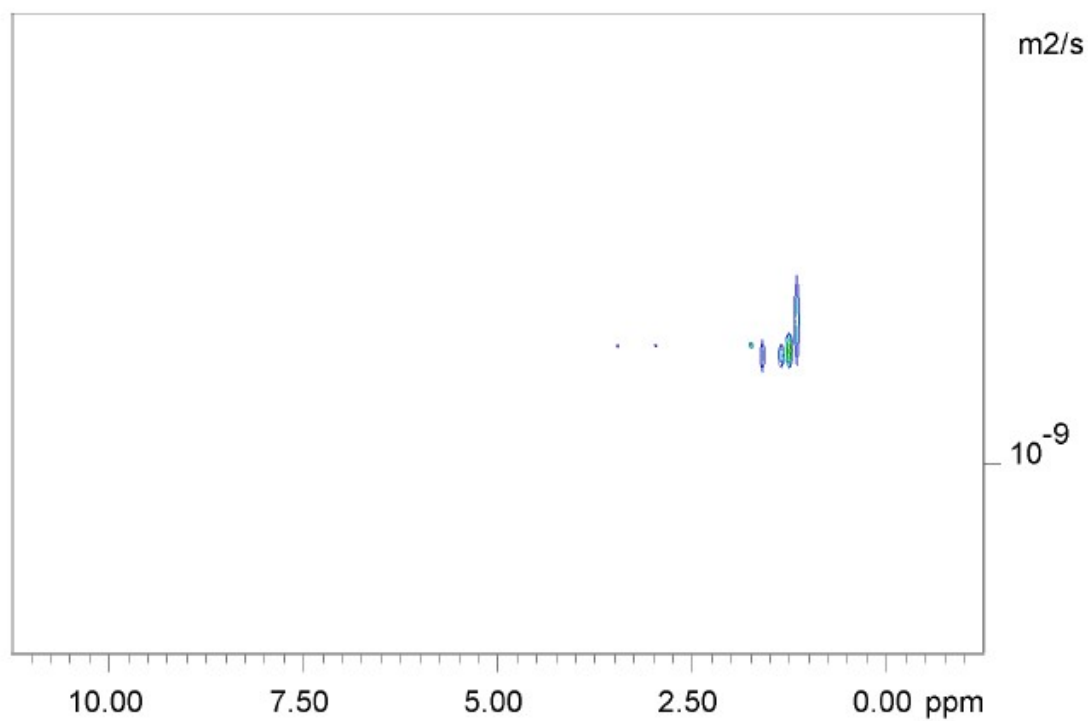


Figure S 10. DOSY spectrum of compound **5** in CDCl_3 .

Supporting Information

^1H NMR spectra of by-products from pyrolysis of compound **3**

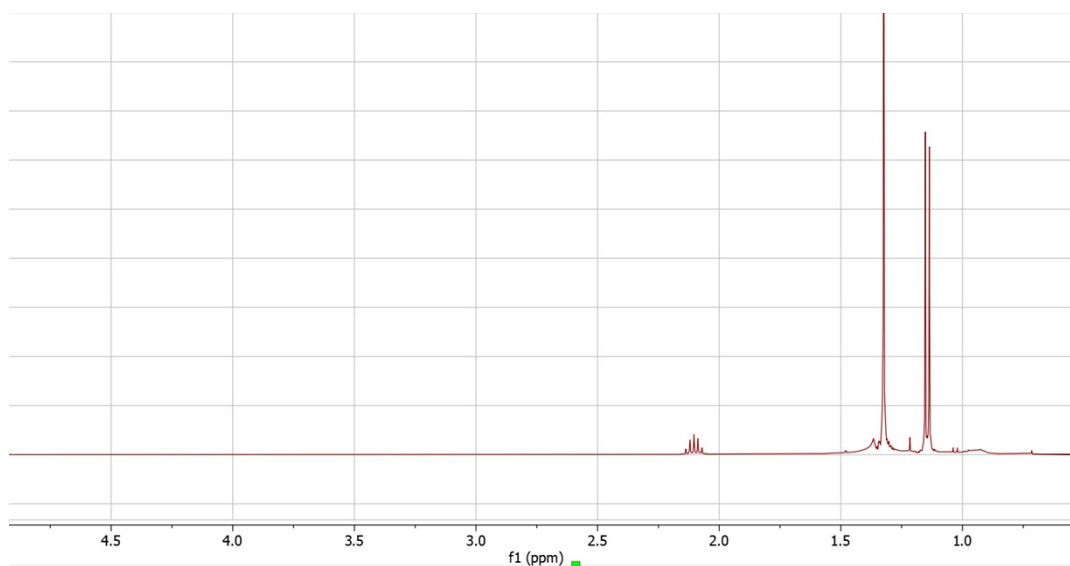


Figure S 11. ^1H NMR spectrum of oil residue from pyrolysis of compound **3** at 250°C.

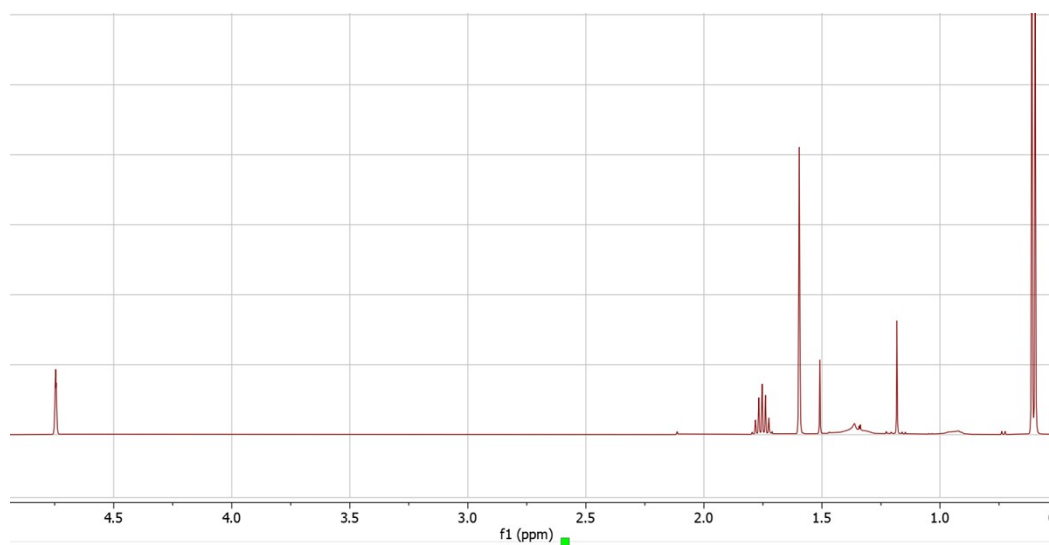


Figure S 12. ^1H NMR spectrum of volatile by-products from pyrolysis of compound **3** at 250°C.

Supporting Information

Energy Dispersive X-Ray spectroscopy Data

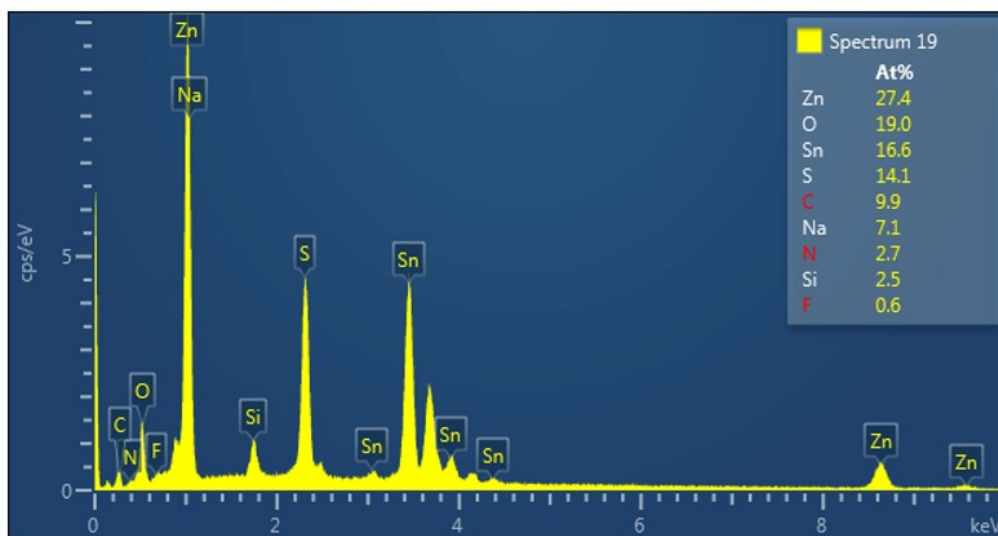


Figure S 13. Example EDX spectrum from analysis of film B.

Table S 2. Tabulated EDX data corresponding to ZnS films A-E

Film	Dep. Temp	Scan number	At % (Zn)	At % (S)	S:Zn Ratio	Average
A	175	1	27.4	14.1	0.514599	
		2	28	14.3	0.510714	
		3	27.4	14.7	0.536496	
B	200	4	26.6	13	0.488722	0.511171
		5	24.9	11.7	0.46988	
		6	28.5	15	0.526316	
		7	28.6	15.2	0.531469	
C	250	1	30.7	24.1	0.785016	0.776881
		2	31.9	25.5	0.799373	
		3	32.1	24.8	0.772586	
		4	32.1	26.2	0.816199	
		5	37.4	26.6	0.71123	
D	300	1	26.9	22.8	0.847584	0.814157
		2	28.4	24.2	0.852113	
		3	28.2	23.4	0.829787	
		4	30	24.3	0.81	
E	350	5	36.1	26.4	0.731302	0.587333
		1	30.1	18.5	0.614618	
		2	29.2	17.6	0.60274	
		3	31.6	18.9	0.598101	
		4	31	17.3	0.558065	
		5	29.3	16.5	0.56314	